Int. J. Environ. Sci. Technol. (2014) 11:1527–1536
DOI 10.1007/s13762-014-0595-y

ORIGINAL PAPER

Clicking graphene oxide and Fe_3O_4 nanoparticles together: an efficient adsorbent to remove dyes from aqueous solutions

M. Namvari · H. Namazi

Received: 14 January 2014 / Revised: 20 March 2014 / Accepted: 21 April 2014 / Published online: 7 May 2014

Abstract Nanohybrid of graphene oxide (GO) and azide-modified Fe_3O_4 nanoparticles (NPs) were fabricated using click reaction. First, Fe_3O_4 NPs were modified by 3-azidopropionic acid. Then, click-coupling of azide-modified Fe_3O_4 NPs with alkyne-functionalized GO was carried out in the presence of $CuSO_4{\cdot}5H_2O$ and sodium L-ascorbate at room temperature. The attachment of Fe_3O_4 NPs onto the graphene nanosheets was confirmed by Fourier-transform infrared (FTIR) spectroscopy, scanning electron microscopy, thermogravimetric analysis, energy dispersive X-ray spectrometry and X-ray diffraction spectrometry. As the FTIR spectroscopy and energy dispersive X-ray spectrometry analysis showed, the final magnetic graphene nanosheets were also reduced by sodium ascorbate which is a merit for click-coupling reactions. The specific saturation magnetization of the Fe_3O_4-clicked GO was 44.3 emu g^{-1}. The synthesized hybrid was used in the adsorption of methylene blue and congo red (CR). The adsorption capacities in the studied concentration range were 109.5 and 98.8 mg g^{-1} for methylene blue and CR, respectively.

Keywords Graphene oxide · Magnetic nanoparticles · Adsorption · Dye removal · Magnetic separation

M. Namvari · H. Namazi (✉)
Laboratory of Dendrimers and Nano-Biopolymers, Faculty of Chemistry, University of Tabriz, P.O. Box 51666, Tabriz, Iran
e-mail: namazi@tabrizu.ac.ir

H. Namazi
Research Center for Pharmaceutical Nanotechnology (RCPN), Tabriz University of Medical Science, Tabriz, Iran

Introduction

Removing toxic metals and dye from the waste water of the manufacturing industries has been of great concern for decades. For this reason, numerous adsorbent with various compositions have been developed (Gupta et al. 2010a, b, c, d, 2012a, b; Gupta and Nayak 2012; Gupta et al. 2011, 2013; Gupta and Saleh 2013; Sanghavi and Srivastava 2013; Ahmaruzzaman and Gupta 2011; Jain et al. 2003; Mittal et al. 2009, 2010). Among them, there has been an increasing attention toward separation process applying magnetic nano-sized particle for adsorption process. Magnetite (Fe_3O_4) nanoparticles (NPs) have attracted a great deal of attention due to a number of unique properties which makes them promising agents as potential materials for carriers of drugs or gene delivery, biomolecules separation, hypothermal treatment of tumors, contrast agents for magnetic resonance imaging, information storage, catalysis and environmental protections such as removing dye and heavy metals (Indira and Lakshmi 2010; Sanghavi et al. 2013a, b; Sanghavi and Srivastava 2010). Graphene, the parent of all graphitic forms including fullerene, carbon nanotubes and graphite, is a two-dimensional building material for carbon materials of all other dimensionalities. Among them, hybrid of graphene and carbon nanotubes with Fe_3O_4 NPs have been extensively studied in the fabrication of functional polymer composites, sensors, waste water treatment, catalysis and drug delivery (He et al. 2010; Lim et al. 2013; Yao et al. 2012). It is believed that hybrid of magnetic NPs and graphene/graphene oxide (GO) would have better functionalities and performances in these applications (Georgakilas et al. 2012; Kumar et al. 2012; Zhu et al. 2013). Recently, Yao et al. have reported the synthesis of magnetic Fe_3O_4@graphene composite which had great potential as an effective adsorbent for removing

cationic and anionic dyes from water solutions (Yao et al. 2012), while Geng et al. have applied a functional hybrid of reduced GO (rGO)–Fe_3O_4 in the adsorption of Rhodamine B (Geng et al. 2012). The mentioned composites showed high efficiency in both cases. However, there are some disadvantages in the process of production and application of these composites: (1) formation of GO–Fe_3O_4 is usually achieved by in situ reduction in iron salt precursors or assembly of the magnetic NPs on GO surface and consequently, Fe_3O_4 NPs are attached to a GO layer only by physical adsorption or electrostatic interaction. Thus, they may be easily leached out from the GO sheets during application (Liu et al. 2008), (2) to prepare Fe_3O_4 NPs by co-precipitation, high temperature is required. For instance, Cong et al. (2010) have prepared magnetic-functionalized rGO sheets through high-temperature decomposition of $Fe(acac)_3$ precursor in polyol, (3) precise controlling the loading amount of Fe_3O_4, and then, tailoring the properties of resultant hybrids for desired application is a main challenge as well (Yang et al. 2009) and (4) another major challenge is because of easy oxidation/dissolution of the pure Fe_3O_4 NPs when using these nanomaterials, specially in acidic solutions. To overcome these problems and specifically to protect the magnetic NPs against oxidation, a shell structure is often introduced, including silica (Zhu et al. 2011a, b) polymer (Shin and Jang 2007) and noble metals (Cho et al. 2005; Lu et al. 2005). And recently, covalent attachment of Fe_3O_4 NPs onto GO has been developed which provides better stability, accessibility, selectivity and less leaching. For example, Fe_3O_4 NPs modified by tetraethyl orthosilicate and (3-aminopropyl) triethoxysilane was reacted with carboxylic groups of GO with the aid of 1-ethyl-3-(3-dimethylaminopropyl) carbodiimide and N-hydroxysuccinimide to form a GO–Fe_3O_4 hybrid and was used to remove neutral red from contaminated water (He et al. 2010). An easy chemical method to produce superparamagnetic GO–Fe_3O_4 hybrid composite and its application in the removal of dyes has also been reported by Xie et al. (2012). In a very recent work, dopamine-functionalized Fe_3O_4 NPs were reacted with GO. The uniqueness of this new and transformative approach was that the NPs provided cellular targeting by an external magnetic field (Yang et al. 2012). A covalent bonding technique to obtain magnetic GO composite (Fe_3O_4/SiO_2–GO) decorated with core/shell NPs has also been reported (Li et al. 2013). Herein, for the first time, we report the covalent attachment of Fe_3O_4 NPs onto GO by powerful and efficient "click reaction". The Cu (I)-catalyzed Huisgen 1, 3-dipolar cycloaddition of azides and terminal alkynes (CuAAC) (Kolb et al. 2001) is significantly an outstanding reaction since it is modular, wide in scope, tolerant to other functional groups, insensitive to solvent, moisture and oxygen. It gives very high yields and only inoffensive by-products that can be easily removed by nonchromatographic methods, and be stereospecific, preferably giving only one product. These are the reasons it has extensively been exploited as a novel methodology to advance drug-discovery, functionalize monolayers, synthesize and functionalize different molecules, polymer, dendrimers, NPs, virus, and to post-translationally engineer proteins and modify cell surfaces (Lahann 2009). In the present work, we developed an efficient method to produce superparamagnetic GO–Fe_3O_4 hybrid using click reaction. Refluxing GO in thionyl chloride ($SOCl_2$) resulted in chlorinated GO (GO–COCl) which was subsequently treated with propargyl alcohol to produce alkyne-GO. Then, 3-azidopropionic acid-functionalized Fe_3O_4 NPs were easily and efficiently clicked onto GO. Covalent attachment of Fe_3O_4 NPs onto GO should be an effective way to solve the problems mentioned above. The adsorption properties of the obtained hybrid (Fe_3O_4-clicked GO) toward methylene blue (MB) as a cationic dye and congo red (CR) as an anionic dye in aqueous solution were investigated as well.

Date and location of the research February and March of 2013, Laboratory of Dendrimers and Nano-Biopolymers, Faculty of Chemistry, University of Tabriz, Tabriz, Iran.

Materials and methods

Graphite (average particle size 30 μm) is commercially available, and it was used without further purification. $SOCl_2$ was distilled from boiled linseed oil prior to use. Triethylamine (Et_3N) and dichloromethane (CH_2Cl_2) were dried over calcium hydride (CaH_2) and then distilled. Tetrahydrofuran (THF) was dried over sodium. 3-bromopropionic acid was recrystallized from carbon tetrachloride. Propargyl alcohol, sodium azide, ferrous chloride tetrahydrate ($FeCl_2{\cdot}4H_2O$), ferric chloride hexahydrate ($FeCl_3{\cdot}6H_2O$), N,N-dimethylformamide (DMF), ethanol, copper sulfate pentahydrate ($CuSO_4{\cdot}5H_2O$) sodium L-ascorbate, MB and CR. All the reagents and solvents employed for the synthesis were commercially available and used as received without further purification unless mentioned. All the reagents, except graphite, were purchased from Merck. Deionized water (DI water) that was used in all experiments.

Instrumentation

Infrared spectra were obtained on a Fourier-transform infrared (FTIR) spectrometer (Bruker Instruments, model Aquinox 55, Germany) in the 4,000–400 cm^{-1} range at a resolution of 0.5 cm^{-1} as KBr pellets. The pattern of X-ray diffraction (XRD) of the samples was obtained by Siemens diffractometer with Cu-ka radiation at 35 kV in the scan

range of 2 h from 2 to 70° and scan rate of 1°/min. Room temperature magnetic properties of the composite were characterized using vibrating sample magnetometer (Iran). Energy dispersive X-ray (EDX) spectrum and scanning electron micrographs (SEM) were obtained using a field-emission scanning electron microscopy (FESEM, MIRA3 FEG-SEM) operating at 10 kV. Thermo gravimetric analysis (TGA) was performed with a TGA-PL thermal analyzer under air atmosphere from room temperature up to 700 °C at a heating rate of 10 °C/min. UV–Vis absorption spectra were recorded on a Shimadzu 1700 Model UV–Vis spectrophotometer.

Preparation of alkyne-GO

The as-prepared GO by modified Hummers' method (Zhang et al. 2010b), (100 mg) was well dispersed in 1 mL of dry DMF by sonification for 1 h and then was treated with $SOCl_2$ (20 mL) at 80 °C for 3 days. After removing the excess of $SOCl_2$ under reduced pressure, propargyl alcohol (2 mL), distilled CH_2Cl_2 (2 mL) and Et_3N (1 mL) were added dropwise to GO at 0 °C. The mixture was stirred at 0 °C for 1 h, at room temperature for 6 h and reflux for 24 h. The powder was washed with an excess amount of ethanol and DI water and dried in vacuo overnight.

Preparation of azide-modified Fe_3O_4 NPs

3-azidopropionic acid was prepared according to the literature (Grandjean et al. 2005) and 1 mL of 3-azidopropionic acid, 10 mg of Fe_3O_4 NPs (Yao et al. 2012) and 5 mL of $CHCl_3$ were added to a centrifuge tube. The resultant mixture was sonicated for 10 min until the NPs were dispersed completely. THF was then added to remove excess of 3-azidopropionic acid. The mixture was washed with ethanol, and the precipitate was collected and dried in vacuo overnight.

Synthesis of Fe_3O_4-clicked GO hybrid by CuAAC reaction

About 10 mg of azide-modified Fe_3O_4 NPs was introduced into 5 mL of mixed solvent of DMF and H_2O (DMF: H_2O 4: 1). Following sonication, 20 mg of alkyne-GO, about 1 mg of $CuSO_4.5H_2O$ and sodium L-ascorbate were added and the mixture was stirred at room temperature overnight. The product was recovered by a magnet and washed with excess of water and ethanol and dried in vacuo overnight.

Adsorption experiments

Effects of contact time and the related isotherms were studied individually. Typically, adsorption experiments were carried out in glass bottles at 25 °C. 25 mL of dye solution of a known initial concentration was shaken with 0.025 g of Fe_3O_4-clicked GO on a shaker at 200 rpm at 25 °C. To evaluate the time effect, at the completion of preset time intervals, a 5 mL dispersion was drawn and separated immediately by the aid of a magnet to collect the adsorbent. The equilibrium concentrations of dyes were measured with a UV–Vis spectrophotometer at the appropriate wavelength corresponding to the maximum absorbance, 664 and 499 nm for MB and CR, respectively. The amount of dye adsorbed was calculated using the following equation:

$$q_e = (C_o - C_e)V/m$$

where, q_e is the concentration of dye adsorbed (mg g^{-1}), C_o and C_e are the initial and equilibrium concentrations of dye in mg L^{-1}, respectively, V is the volume of dye solution (L) and m (g) is the weight of the adsorbent used.

For adsorption equilibrium experiments, fixed adsorbent dose (25 mg) was weighed into 50 mL conical flasks containing 25 mL of different initial concentrations (20–120 mg L^{-1}) of the related dye. The mixture was shaken for 5 h at 25 °C until equilibrium was obtained. Then, the adsorbent was separated from solution by an external magnet. The concentration of the dye in the solution was measured using a UV–Vis spectrophotometer.

Results and discussion

In this study, we report the covalent attachment of superparamagnetic Fe_3O_4 NPs onto GO through click reaction between 3-azidopropionic acid coated-Fe_3O_4 NPs and propargyl-functionalized GO as described in Fig. 1. The application of the powerful and efficient click reaction in covalent bonding of NPs onto GO is reported for the first time in this paper. Nano-sized particles tend to aggregate to minimize their surface energy due to their large ratio of surface area per unit volume. Therefore, to achieve stability, NPs are usually functionalized with specific groups, for instance surfactants, polysaccharides, zeolite, activated carbon and cyclodextrin. The coating method can also hamper the aggregation of the particles at a distance where the attraction energy between the particles is larger than the disordering energy of thermal motion (Nigam et al. 2011). Carboxylates such as citric acid (Namazi et al. 2011; Namazi and Adeli 2003) can suitably stabilize Fe_3O_4 NPs (Cheraghipour et al. 2012). Thus, we decided to use 3-azidopropionic acid to cap the NPs which was achieved by ultrasonication. Then, azide-modified NPs were clicked onto the edges of GO to result the final product (Fe_3O_4-clicked GO).

The superparamagnetic behavior of Fe_3O_4-clicked GO was verified using an external magnet as shown in Fig. 2.

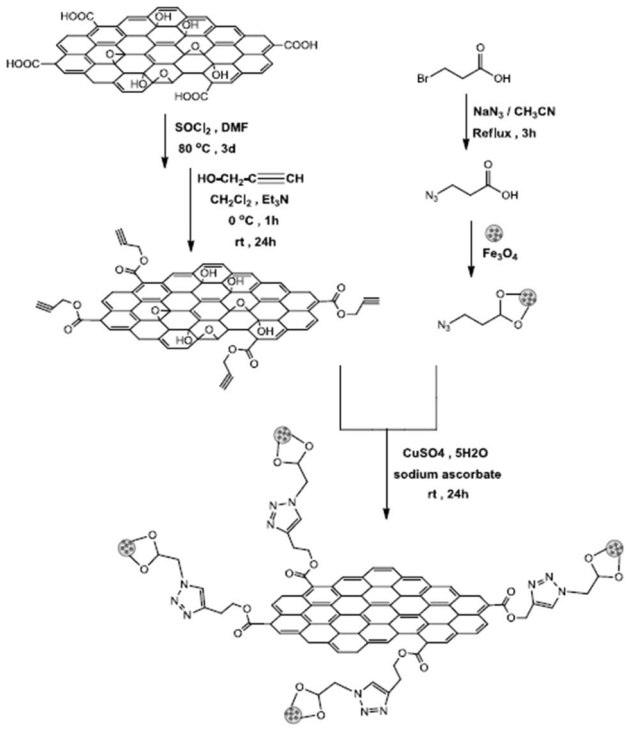

Fig. 1 General procedure for the preparation of Fe_3O_4-clicked GO

Fig. 2 Photo image of response of Fe_3O_4-clicked GO to an external magnetic field

When a magnet is placed close to the vial containing Fe_3O_4-clicked GO, the nanohybrid readily aggregates to the wall of the vial which proves that the azide-modified Fe_3O_4 NPs have successfully attached onto GO and it is consequently magnetically responsive.

Characterization of the synthesized materials by FTIR was performed to confirm the accomplishment of each step. The FTIR spectra of GO, alkyne-GO, 3-azidopropionic acid, azide-modified Fe_3O_4 NPs and Fe_3O_4-clicked GO are shown in Fig. 3. The presence of several characteristic peaks of GO such as C=O (1,735 cm^{-1}), aromatic C=C (1,626 cm^{-1}) and alkoxy C–O (1,074 cm^{-1}) stretching confirms the successful oxidation of graphite and is in good agreement with previous reports (Yang et al. 2012). In the FTIR spectrum of alkyne-GO, the new signals at 1,745 cm^{-1} (C=O of ester), 2,150 cm^{-1} of (C≡C stretch of alkyne), 2,874 cm^{-1} (aliphatic hydrogens) and 3,027 cm^{-1}(≡C–H stretch of alkyne) prove the attachment of alkyne groups onto the edges of GO. In addition, there is no sign of the stretching signals of CO–H which indicates that the carboxylic acid groups have changed into ester functionality (Ryu et al. 2013). A sharp absorption band at 2,105 cm^{-1} in the FTIR spectrum of azide-modified Fe_3O_4 NPs, is attributed to azide stretching signal that shows the formation of 3-azidopropionic acid. Fe_3O_4 NPs were attached to 3-azidopropionic acid with ultrasonication. The appearance of a signal at 570 cm^{-1} which is attributed to Fe_3O_4 NPs and more importantly, the absence of peaks at 1,719 and 3,374 cm^{-1}, assigned to stretching of the C=O and CO–H of carboxyl groups, respectively, in the FTIR spectrum of azide-modified Fe_3O_4 NPs is strong confirmations to the attachment of Fe_3O_4 NPs to 3-azidopropionic acid. The disappearance of the characteristic peaks related to alkyne and azide moieties in the FTIR spectrum of Fe_3O_4-clicked GO indicates that the starting materials no more exist. Besides, the upcoming new band at 1,646 cm^{-1}, which is attributed to the triazole group and the presence of the peaks of azide-modified Fe_3O_4 NPs, prove that the click reaction was carried out and the Fe_3O_4 NPs were successfully attached covalently onto GO. Besides, ascorbic acid has been reported to be an effective reducing agent for GO than can compete with hydrazine (Zhang et al. 2010a). As it is obvious from the FTIR spectrum of the nanohybrid, the stretching band of O–H and epoxy are not present which indicates that during click reaction, GO has been reduced as well. This is an added advantage for click-coupling reactions.

The XRD patterns of GO, alkyne-GO, azide-modified Fe_3O_4 and Fe_3O_4-clicked GO are presented in Fig. 4. Oxidation generates oxygen-containing groups on the originally atomically flat graphene sheets which makes individual GO sheets thicker than individual pristine graphene sheets (Shen et al. 2010) thus, GO shows a sharp (0 0 1) peak at 10.44°. Alkyne- functionalized GO shows a XRD pattern similar to GNS, and the related peak is seen at $2\theta = 24.11°$. Besides, the (0 0 1) peak of GO is barely there. This indicates that layered GO has been exfoliated (Shen et al. 2010). For azide-functionalized Fe_3O_4, diffraction peaks with 2θ at 30.21°, 35.58°, 43.35°, 53.30°, 57.10° and 62.57° were observed and are attributed to the (2 2 0), (3 1 1), (4 0 0), (4 2 2), (5 1 1) and (4 4 0) planes of the Fe_3O_4. The pattern was in accord with pure spinel Fe_3O_4 (ICDD file no. 65-3107), indicative of a cubic spinel structure of the magnetite. Compared with azide-modified

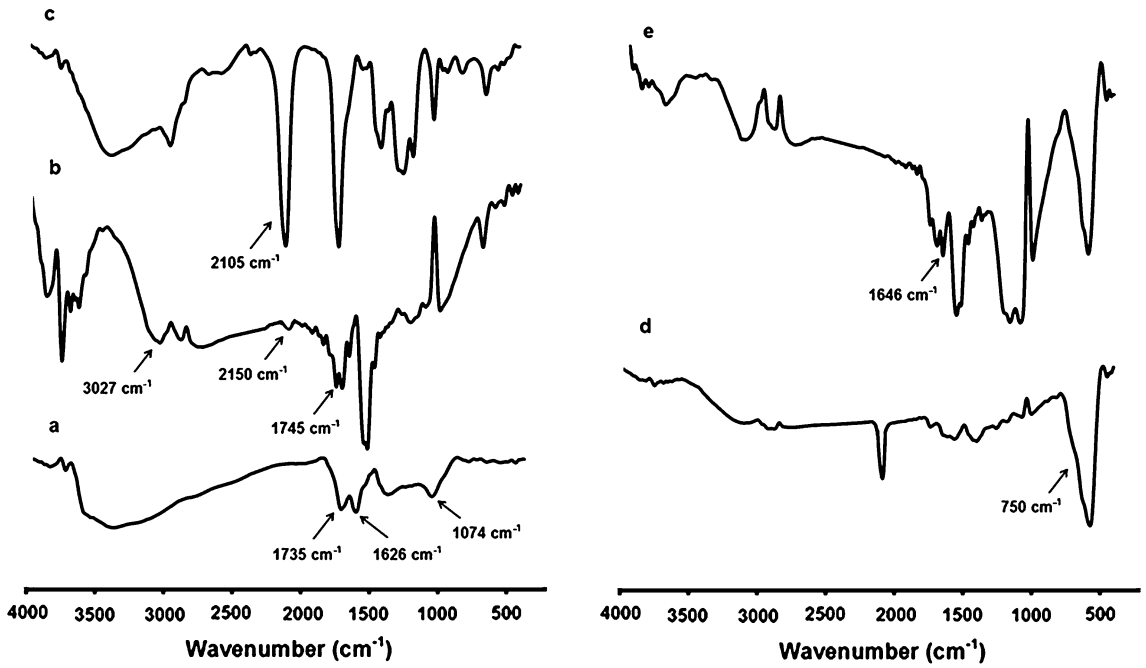

Fig. 3 The FTIR spectra of GO (**a**), alkyne-GO (**b**), 3-azidopropionic acid (**c**), azide-modified Fe_3O_4 NPs (**d**) and Fe_3O_4-clicked GO (**e**)

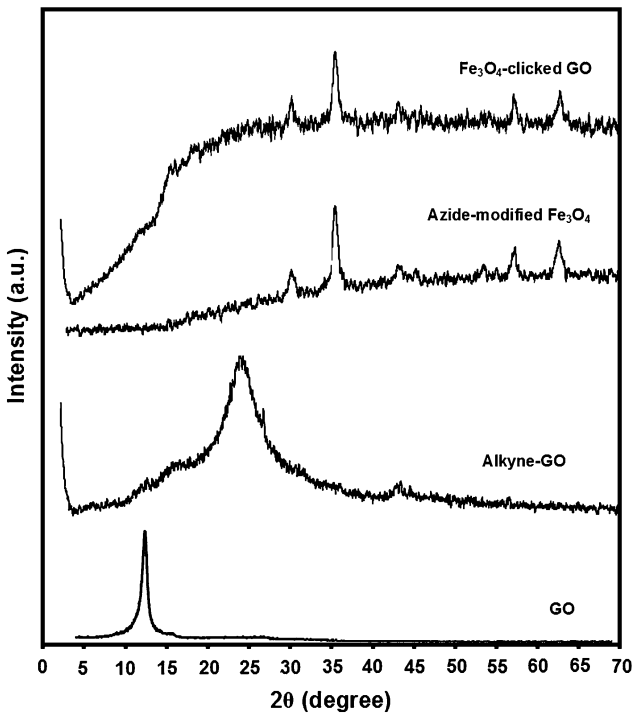

Fig. 4 The XRD patterns of GO, alkyne-GO, azide-modified Fe_3O_4 and Fe_3O_4-clicked GO

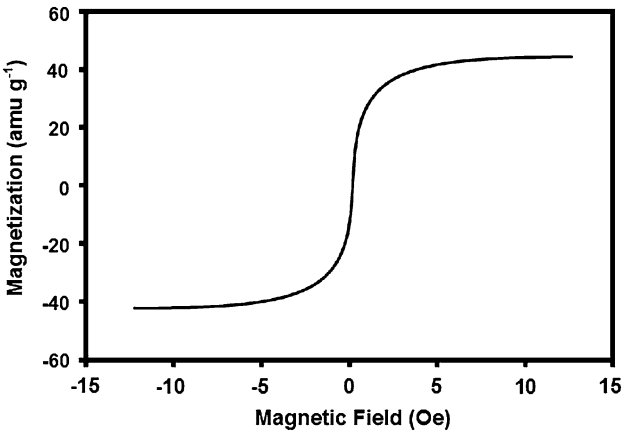

Fig. 5 Magnetization curve of Fe_3O_4-clicked GO

Fe_3O_4, the same set of characteristic peaks was also observed for Fe_3O_4-clicked GO indicating the stability of the crystalline phase of Fe_3O_4 NPs in the nanohybrid (Li et al. 2013) and confirming the attachment of NPs onto and confirming the attachment of NPs onto GO. The diffraction peak of alkyne-GO has disappeared which suggests that alkyne-GO layers have been exfoliated and less agglomerated graphene sheet are present in the nanohybrid (Yao et al. 2012).

The magnetization curve of Fe_3O_4-clicked GO was measured at room temperature and is presented in Fig. 5. The magnetic hysteresis loop is S-like curve. The saturation magnetization (Ms) is 44.3 emu g^{-1}. The prepared hybrid exhibited zero coercivity and permanence indicating its superparamagnetism.

To investigate the morphology and structure of the products, FESEM images were taken for the azide-modified Fe_3O_4 NPs and Fe_3O_4-clicked GO. Figure 6a and b shows the FESEM images of azide-modified Fe_3O_4 NPs

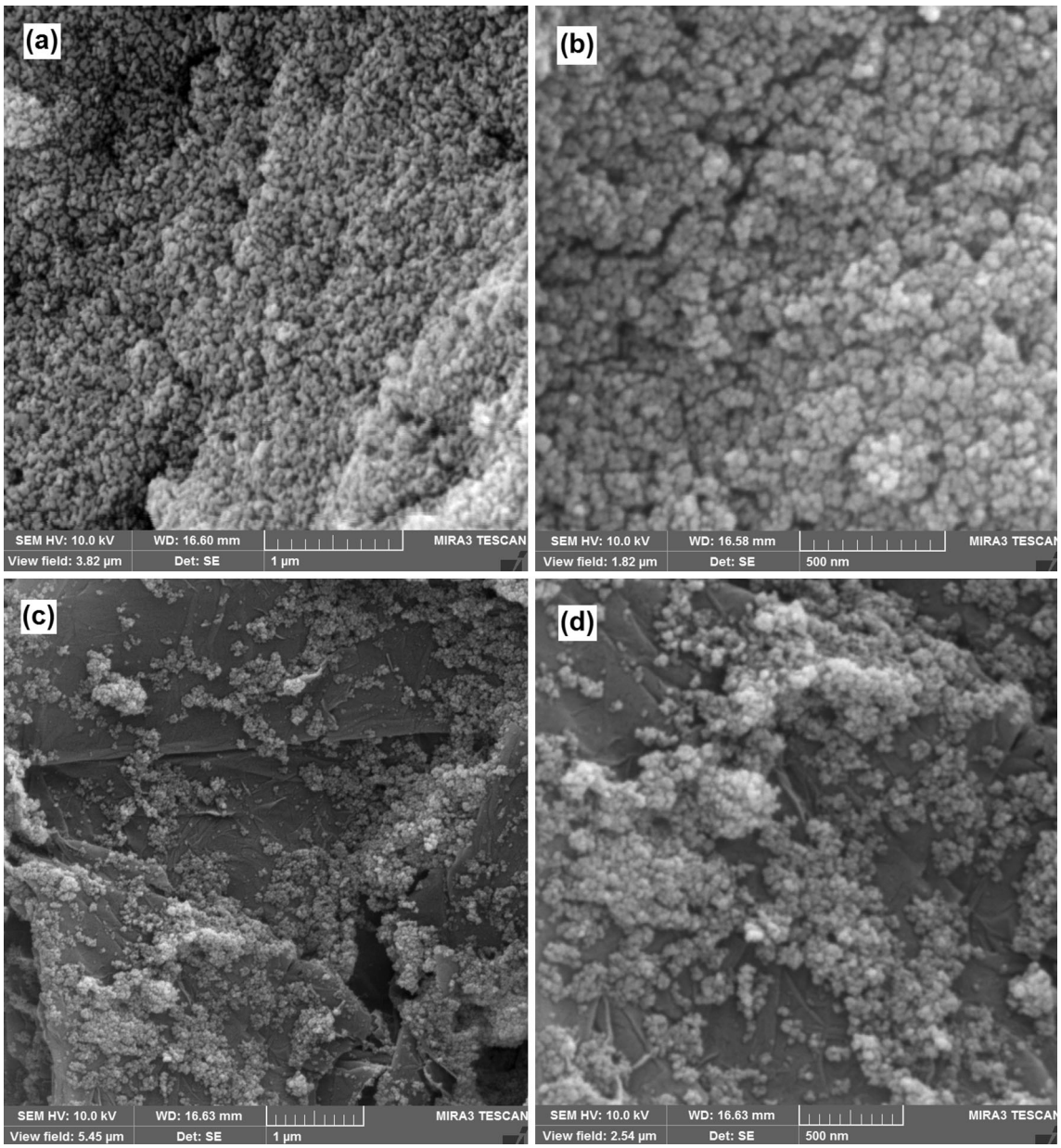

Fig. 6 FESEM images of azide-modified Fe_3O_4 NPs (**a**, **b**) and Fe_3O_4-clicked GO (**c**, **d**)

in which the granular nature of the NPs is clearly observed with gray/white color on their surface indicating the azidopropionic acid coating. Homogeneous distribution of the Fe_3O_4 NPs is obvious. Figure 5c and d confirms the attachment of Fe_3O_4 NPs onto GO. The layer-by-layer assembly of magnetic GO sheets is clearly observed.

Furthermore, the composition of this heterostructure is confirmed by the EDX spectroscopy experiment (Fig. 7) which reveals the presence of intense peaks for Fe along with carbon and oxygen peaks. This clearly shows the grafting of Fe_3O_4 onto GO. In addition, low content of oxygen given by this analysis also proves the reduction in GO sheets by sodium ascorbate.

TG analysis was also conducted on GO, azide-modified Fe_3O_4, and Fe_3O_4-clicked GO (Fig. 8) to distinguish and access thermal stability as well as to confirm the attachment of azide-modified Fe_3O_4 NPs onto GO. GO exhibits two steps of mass loss, first one before 120 °C which is attributed to the evaporation of adsorbed water and the main step up to 400 °C is related to the decomposition of oxygen-containing functional groups such as carboxyl, hydroxyl and epoxy (Yang et al. 2012). In the TGA diagram of azide-modified Fe_3O_4 NPs, weight loss of 1.2 %

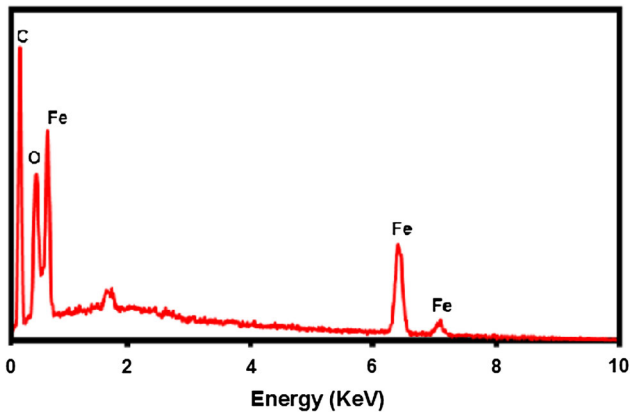

Fig. 7 EDX spectrum of Fe_3O_4-clicked GO

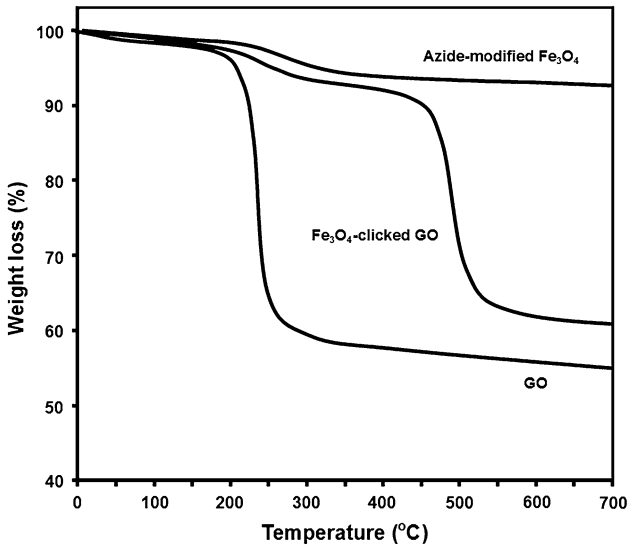

Fig. 8 TGA curves of GO, azide-modified Fe_3O_4, and Fe_3O_4-clicked GO

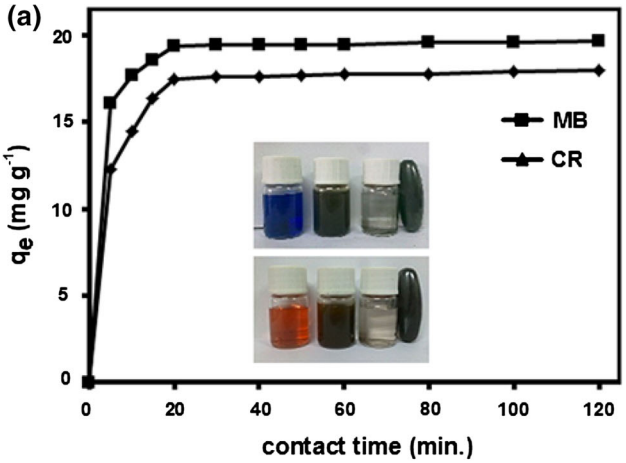

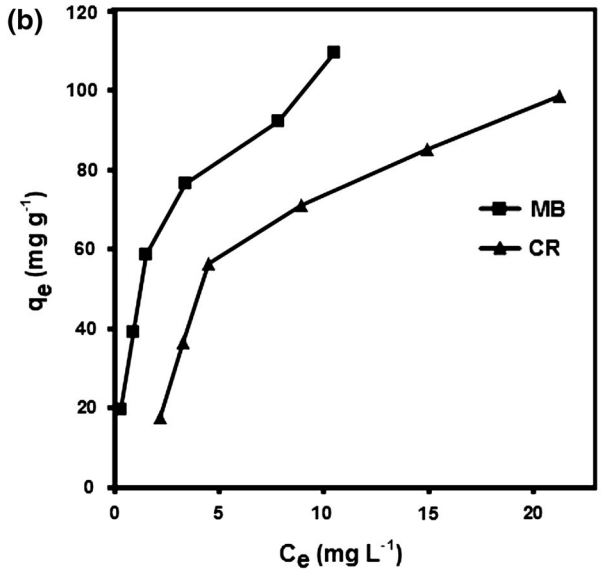

Fig. 9 The effect of contact time on the adsorption of dyes onto the Fe_3O_4-clicked GO hybrid (**a**). *Inset* shows photos of Fe_3O_4-clicked GO hybrid: initial solution of dye (*left*), solution of the adsorbent and dye (*middle*) and the response of the solution of the adsorbent and dye to a magnet (*right*), (Experimental conditions: temperature: 25 °C, adsorbent dose: 25 mg/25 mL, initial concentration of dyes: 20 mg L^{-1}) and adsorption isotherms of dyes onto the Fe_3O_4-clicked GO hybrid (**b**)

can be assigned to the removal of water which is seen below 140 °C and the weight loss of 5.0 % between 140 and 418 °C can be due to the loss of 3-azidopropionic acid groups. The pattern and the percentage of weight loss of azide-modified Fe_3O_4 NPs totally differ from the pristine Fe_3O_4 NPs (Ma et al. 2012), and this confirms that the azidopropionic acid molecules have well covered the surface of Fe_3O_4 NPs which prevents the exposure of thermally labile hydroxyl functional groups of Fe_3O_4 NPs (Yang et al. 2014). TG analysis of Fe_3O_4-clicked GO presents that the nanohybrid undergoes three stages of thermal degradation. The first stage with the weight loss of 7.8 % is observed between 150 and 370 °C. The main step which is seen between 370 and 550 °C with the mass loss of 31 % can be attributed to the decomposition of triazole group. And the final stage happening after 550 °C is 4.9 % and is related to the decomposition of carbon skeleton. Besides, the mass loss over the whole temperature of 500–700 °C is low demonstrating the high efficiency of the covalent functionalization (Shen et al. 2010).

Adsorption studies

The adsorption of dyes MB and CR from aqueous solutions using the synthesized hybrid was studied. The effect of contact time on the amount of dye adsorbed was investigated at an initial concentration of 20 mg L^{-1} of both dyes (Fig. 9a). It only took 20 min for both dyes to reach equilibrium. The short equilibrium time needed indicates

Table 1 Maximum adsorption capacities for the adsorption of MB onto various adsorbents

Adsorbent	Adsorption capacity (mg g^{-1})	References
GO–Fe_3O_4 hybrid	167.2	Xie et al. (2012)
Na-ghassoulite	135	Xie et al. (2009)
Kaolinite	76.9	Hu et al. (2011)
Activated carbon	521	Juang et al. (2000)
Magnetic Fe_3O_4@graphene	45.27	Yao et al. (2012)
MWCNTs with Fe_2O_3	42.3	Qu et al. (2008)
GNS/Fe_3O_4 composite	35.73	Aia et al. (2011)
TiO_2–GNs	83.3	Thuy-Duong et al. (2012)
CNT–GNs	81.97	Ai and Jiang (2012)
Fe_3O_4-clicked GO	109.5	This work

Table 2 Maximum adsorption capacities for the adsorption of CR onto various adsorbents

Adsorbent	Adsorption capacity (mg g^{-1})	References
Magnetic cellulose/Fe_3O_4/activated carbon	66.09	Zhu et al. (2011a, b, c)
N,O-carboxymethyl-chitosan montmorillonite	74.24	Wang and Wang (2008)
Waste red mud	4.05	Namasivayam and Arasi (1997)
Chitosan/montmorillonite	54.52	Wang and Wang (2007)
Magnetic Fe_30_4@graphene	33.66	Yao et al. (2012)
Fe_3O_4-clicked GO	98.8	This work

that the hybrid has high adsorption efficiency to remove cationic and anionic dyes from contaminated water. The obtained results are better than the ones reported previously (Yao et al. 2012; Xie et al. 2012).

The adsorption isotherms of MB and CR for the hybrid are shown in Fig. 9b. To study the distribution of the adsorption molecules between the liquid phase and solid phase at the equilibrium state, the adsorption isotherm is used. The maximum adsorption capacity was attained 109.5 and 98.8 mg g^{-1} for MB and CR, respectively, at an initial concentration of 20 mg L^{-1}. The obtained result is comparable with the previous reports (Yao et al. 2012; Xie et al. 2012).

Tables 1 and 2 show the results obtained in this study with those in the previously reported works on adsorption capacities of various adsorbent in aqueous solution for MB.

Conclusion

The covalent attachment of NPs onto the GO surface using the powerful click reaction is reported for the first time. Not only this nanohybrid was prepared in an ambient condition, but also the magnetic GNS were reduced by sodium ascorbate during click-coupling reaction which was confirmed by FTIR and EDX. The covalent attachment of Fe_3O_4 NPs onto GO, being able to predefine the loading amount of Fe_3O_4 NPs and less leaching are of other outstanding advantages of this method. The attachment of Fe_3O_4 NPs onto the GNS was confirmed by FTIR, FESEM, XRD, TGA and EDX. The specific saturation magnetization of the Fe_3O_4-clicked GO was 44.3 emu g^{-1}. The synthesized hybrid was used in the adsorption of MB and CR. The adsorption capacities in the concentration range studied were 109.5 and 98.8 mg g^{-1} for MB and CR, respectively. High adsorption capacity, compared with other adsorbents, accompanied by the ease of separation by an external magnetic field makes the prepared nanohybrid a powerful separation tool to be utilized in wastewater treatment.

Acknowledgments Authors are pleased to acknowledge the University of Tabriz and Research Center for Pharmaceutical Nanotechnology (RCPN), Tabriz University of Medical Science for financial support of this work.

References

Ahmaruzzaman M, Gupta VK (2011) Rice husk and its ash as low-cost adsorbents in water and wastewater treatment. Ind Eng Chem Res 50:13589–13613

Ai L, Jiang J (2012) Removal of methylene blue from aqueous solution with self-assembled cylindrical graphene–carbon nanotube hybrid. Chem Eng J 192:156–163

Aia L, Zhang C, Chen Z (2011) Removal of methylene blue from aqueous solution by a solvothermal-synthesized graphene/magnetite composite. J Hazard Mater 192:1515–1524

Cheraghipour E, Javadpour S, Mehdizadeh AR (2012) Citrate capped superparamagnetic iron oxide nanoparticles used for hyperthermia therapy. J Biomed Sci Eng 5:715–719

Cho SJ, Idrobo JC, Olamit J, Liu K, Browning ND, Kauzlarich SM (2005) Growth mechanisms and oxidation resistance of gold-coated iron nanoparticles. Chem Mater 17:3181–3186

Cong HP, He JJ, Lu Y, Yu SH (2010) Water-soluble magnetic functionalized reduced graphene oxide sheets: in situ synthesis and magnetic resonance imaging applications. Small 6:169–173

Geng Zh, Lin Y, Yu X, Shen Q, Ma L, Li Zh et al (2012) Highly efficient dye adsorption and removal: a functional hybrid of reduced graphene oxide–Fe_3O_4 nanoparticles as an easily regenerative adsorbent. J Mater Chem 22:3527–3535

Georgakilas V, Otyepka M, Bourlinos AB, Chandra V, Kim N, Kemp KC et al (2012) Functionalization of graphene: covalent and non-covalent approaches, derivatives and applications. Chem Rev 112:6156–6214

Grandjean C, Boutonnier A, Guerreiro C, Fournier J-M, Mulard LA (2005) On the preparation of carbohydrate-protein conjugates using the traceless Staudinger ligation. J Org Chem 70:7123–7132

Gupta VK, Nayak A (2012) Cadmium removal and recovery from aqueous solutions by novel adsorbents prepared from orange peel and Fe_2O_3 nanoparticles. Chem Eng J 180:81–90

Gupta VK, Saleh TA (2013) Sorption of pollutants by porous carbon, carbon nanotubes and fullerene-An overview. Environ Sci Pollut Res 20:2828–2843

Gupta VK, Jain R, Malathi S, Nayak A (2010a) Adsorption-desorption studies of indigocarmine from industrial effluents by using deoiled mustard and its comparison with charcoal. J Colloid Interface Sci 384:628–633

Gupta VK, Jain R, Shrivastava M, Nayak A (2010b) Equilibrium and thermodynamic studies on the adsorption of the dye Tartrazine onto waste "Coconut Husks" carbon and activated carbon. J Chem Eng Data 55:5083–5090

Gupta VK, Rastogi A, Nayak A (2010c) Adsorption studies on the removal of hexavalent chromium from aqueous solution using a low cost fertilizer industry waste material. J Colloid Interface Sci 342:135–141

Gupta VK, Rastogi A, Nayak A (2010d) Biosorption of nickel onto treated alga (Oedogonium hatei): application of isotherm and kinetic models. J Colloid Interface Sci 342:533–539

Gupta VK, Agarwal Sh, Saleh TA (2011) Synthesis and characterization of alumina-coated carbon nanotubes and their application for lead removal. J Hazard Mater 185:17–23

Gupta VK, Ganjali MR, Nayak A, Bhushan B, Agarwal Sh (2012a) Enhanced heavy metals removal and recovery by mesoporous adsorbent prepared from waste rubber tire. Chem Eng J 197:330–342

Gupta VK, Nayak A, Agarwal Sh, Dobhal R, Uniyal DP, Singh P (2012b) Arsenic speciation analysis and remediation techniques in drinking water. Desalin Water Treat 40:231–243

Gupta VK, Pathania D, Agarwal S, Sharma S (2013) Removal of Cr(VI) onto Ficus carica biosorbent from water. Environ Sci Pollut Res 20:2632–2644

He F, Fan J, Ma D, Zhang L, Leung C, Chan HL (2010) The attachment of Fe_3O_4 nanoparticles to graphene oxide by covalent bonding. Carbon 48:3139–3144

Hu YW, Li FH, Bai XX, Li D, Hua SC, Wang KK et al (2011) Catalytic performance of plate-type Cu/Fe nanocomposites on ZnO nanorods for oxidative steam reforming of methanol. Chem Commun 47:1473–1475

Indira TK, Lakshmi PK (2010) Magnetic nanoparticles—a review. Int J Pharm Sci Nanotechnol 3:1035–1042

Jain AK, Gupta VK, Bhatnagar A, Suhas A (2003) Comparative study of adsorbents prepared from industrial wastes for removal of dyes. Sep Sci Technol 38:463–481

Juang RS, Wu FC, Tseng RL (2000) Mechanism of adsorption of dyes and phenols from water using activated carbons prepared from plum kernels. J Colloid Interface Sci 227:437–444

Kolb HC, Finn MG, Sharpless KB (2001) Click chemistry: diverse chemical function from a few good reactions. Angew Chem Int Ed 40:2004–2021

Kumar R, Singh RK, Dubey PK, Oh I-K (2012) Review on functionalized graphenes and their applications. Smart Nanosyst Eng Med 1:18–39

Lahann J (ed) (2009) Click chemistry for biotechnology and materials science. Wiley, UK

Li H, Chi Z, Li J (2013) Covalent bonding synthesis of magnetic graphene oxide nanocomposites for Cr(III) removal. Desalin Water Treat 52:1–10

Lim HN, Huang NM, Chia CH, Harrison I (2013) Inorganic nanostructures decorated graphene. In: Ferreira SO (ed) Advanced topics on crystal growth. CC BY 3.0 license; 2013, ISBN: 978-953-51-1010-1, InTech. doi:10.5772/54321

Liu QF, Ren WC, Chen ZG, Liu BL, Yu B, Li F (2008) Direct synthesis of carbon nanotubes decorated with size-controllable Fe nanoparticles encapsulated by graphitic layers. Carbon 46:1417–1423

Lu ZH, Prouty MD, Guo ZH, Golub VO, Kumar C, Lvov YM (2005) Magnetic switch of permeability for polyelectrolyte microcapsules embedded with Co@Au nanoparticles. Langmuir 21:2042–2050

Ma Y-X, Li Y-F, Zhao G-H, Yang L-Q, Wang J-Z, Shan X et al (2012) Preparation and characterization of graphite nanosheets decorated with Fe_3O_4 nanoparticles used in the immobilization of glucoamylase. Carbon 50:2976–2986

Mittal A, Mittal J, Malviya A, Gupta VK (2009) Adsorptive removal of hazardous anionic dye "Congo red" from wastewater using waste materials and recovery by desorption. J Colloid Interface Sci 340:16–26

Mittal A, Mittal J, Malviya A, Gupta VK (2010) Removal and recovery of Chrysoidine Y from aqueous solutions by waste materials. J Colloid Interface Sci 344:497–507

Namasivayam C, Arasi DJSE (1997) Removal of congo red from wastewater by adsorption onto waste red mud. Chemosphere 34:401–417

Namazi H, Adeli M (2003) Novel linear–globular thermoreversible hydrogel ABA type copolymers from dendritic citric acid as the A blocks and poly(ethyleneglycol) as the B block. Eur Polym J 39:1491–1500

Namazi H, Motamedi S, Namvari M (2011) Synthesis of new functionalized citric acid-based dendrimers as nanocarrier agents for drug delivery. BioImpacts 1:63–69

Nigam S, Barick KC, Bahadur D (2011) Development of citrate-stabilized Fe_3O_4 nanoparticles: conjugation and release of doxorubicin for therapeutic applications. J Magn Magn Mater 323:237–243

Qu S, Huang F, Yu SN, Chen G, Kong JL (2008) Magnetic removal of dyes from aqueous solution using multi-walled carbon nanotubes filled with Fe_2O_3 particles. J Hazard Mater 160:643–647

Ryu HJ, Mahapatra SS, Yadav SK, Cho JW (2013) Synthesis of click-coupled graphene sheet with chitosan: effective exfoliation and enhanced properties of their nanocomposites. Eur Polym J 49:2627–2634

Sanghavi BJ, Srivastava AK (2010) Simultaneous voltammetric determination of acetaminophen, aspirin and caffeine using an in situ surfactant-modified multiwalled carbon nanotube paste electrode. Electrochim Acta 55:8638–8648

Sanghavi BJ, Srivastava AK (2013) Adsorptive stripping voltammetric determination of imipramine, trimipramine and desipramine employing titanium dioxide nanoparticles and an Amberlite XAD-2 modified glassy carbon paste electrode. Analyst 138:395–1404

Sanghavi BJ, Kalambate PK, Srivastava AK (2013a) Voltammetric determination of sumatriptan based on a graphene/gold nanoparticles/Nafion composite modified glassy carbon electrode. Talanta 120:1–9

Sanghavi BJ, Sitaula S, Griep MH, Karna SP, Ali MF, Swami NS (2013b) Real-time electrochemical monitoring of adenosine triphosphate in the picomolar to micromolar range using graphene-modified electrodes. Anal Chem 85:8158–8165

Shen J, Li N, Shi M, Hu Y, Ye M (2010) Covalent synthesis of organophilic chemically functionalized graphene sheets. J Colloid Interface Sci 348:377–383

Shin S, Jang J (2007) Thiol containing polymer encapsulated magnetic nanoparticles as reusable and efficiently separable adsorbent for heavy metal ions. Chem Commun 41:4230–4232

Thuy-Duong NP, Viet Hung P, Kim EJ, Oh ES, Hur SH, Chung JS et al (2012) Reduced graphene oxide–titanate hybrids: morphologic evolution by alkali-solvothermal treatment and applications in water purification. Appl Surf Sci 258:4551–4557

Wang L, Wang A (2007) Adsorption characteristics of Congo Red onto the chitosan/montmorillonite nanocomposite. J Hazard Mater 147:979–985

Wang L, Wang A (2008) Adsorption behaviors of Congo red on the N, O-carboxymethyl-chitosan/montmorillonite nanocomposite. Chem Eng J 143:43–50

Xie LM, Ling X, Fang Y, Zhang J, Liu ZF (2009) Graphene as a substrate to suppress fluorescence in resonance Raman spectroscopy. J Am Chem Soc 131:9890–9891

Xie G, Xi P, Liu H, Chen F, Huang L, Zeng Zh et al (2012) A facile chemical method to produce superparamagnetic graphene oxide–Fe_3O_4 hybrid composite and its application in the removal of dyes from aqueous solution. J Mater Chem 22:1033–1039

Yang XY, Zhang XY, Ma YF, Huang Y, Wang YS, Chen YS (2009) Superparamagnetic graphene oxide–Fe_3O_4 nanoparticles hybrid for controlled targeted drug carriers. J Mater Chem 19:2710–2714

Yang Q, Pan X, Clarke K, Li K (2012) Covalent functionalization of graphene with polysaccharides. Ind Eng Chem Res 51:310–317

Yang JH, Ramaraj B, Yoon KR (2014) Preparation and characterization of superparamagnetic graphene oxide nanohybrids anchored with Fe_3O_4 nanoparticles. J Alloys Compd 583:128–133

Yao Y, Miao S, Liu S, Ma LP, Sun H, Wang S (2012) Synthesis, characterization, and adsorption properties of magnetic Fe_3O_4@graphene nanocomposite. Chem Eng J 184:326–332

Zhang J, Yang H, Shen G, Cheng P, Zhang J, Guo SH (2010a) Reduction of graphene oxide via L-ascorbic acid. Chem Commun 46:1112–1114

Zhang K, Zhang LL, Zhao XS, Wu J (2010b) Graphene/polyaniline nanofiber composites as supercapacitor electrodes. Chem Mater 22:1392–1401

Zhu JH, Wei SY, Haldolaarachchige N, Young DP, Guo ZH (2011a) Electromagnetic field shielding polyurethane nanocomposites reinforced with core-shell Fe-silica nanoparticles. J Phys Chem C 115:15304–15310

Zhu H-Y, Fu Y-Q, Jiang R, Jiang J-H, Xiao L, Zeng G-M et al (2011b) Adsorption removal of congo red onto magnetic cellulose/Fe_3O_4/activated carbon composite: equilibrium, kinetic and thermodynamic studies. Chem Eng J 173:494–502

Zhu J, Chen M, He Q, Shao L, Wei S, Guo Zh (2013) An overview of the engineered graphene nanostructures and nanocomposites. RSC Adv 3:22790–22824